7A.3 FALL VELOCITY SPECTRUM IN THE MELTING LAYER AT KU-BAND

Merhala Thurai*, Hiroshi Hanado and Toshio Iguchi
Communications Research Laboratory, Tokyo, Japan

1. INTRODUCTION

The rain profiling algorithm used for the TRMM precipitation radar (PR) relies on the attenuation at Ku-band being estimated accurately (Iguchi et al 2000). In stratiform rain, the attenuation correction procedure makes a distinction between rain and the melting layer and their respective attenuations are treated differently. For the latter case, the bright-band model as described by Awaka et al. (1985) is used in order to calculate the specific attenuation for each range gate containing the melting particles. The attenuation is evaluated on a profile by profile basis.

The melting layer attenuation – if estimated incorrectly – can lead to inaccuracies in the retrieved surface rainfall rates. A consistent over-estimation or under-estimation of this attenuation will result in a bias in the rainfall estimates. Since the radar only measures the co-polar backscatter reflectivity, the chosen bright band model should not only be sufficiently accurate but also require the measured reflectivity as its only input data. Hence, despite the fact that there are many melting layer models, (e.g. Hardaker et al (1995), Russchenberg and Ligthart (1996), D'Amico et al (1998), Liao et al (2002)), the current rain retrieval algorithm for the TRMM – PR utilizes the relatively simple "Non-coalescence – Non-break up" (N-N) model for deriving the attenuation corrections.

A previous study conducted in the tropics used long-term measurements from an S-band vertically-pointing Doppler radar to examine the accuracy of the N-N model (Thurai et al 2003). From the averaged reflectivity (dBZ) and Doppler profiles measured with a range resolution of 75 meters, it was possible to compare the model-predictions based only on the rainfall rate just below the melting layer. The comparisons were made in terms of the dBZ, the mean fall velocity and the spectrum-width profiles predicted by the model. Very good agreement was obtained in all three parameters.

This paper examines the melting layer characteristics at Ku-band, using data from a multi-parameter Doppler radar operating at 13.8 GHz. The radar operated in the vertically-pointing mode. We report here the fall velocity spectra derived from the radar measurements and the comparisons with those extracted from the N-N model.

**Corresponding author address:* Merhala Thurai, Precipitation Radar Group, Communications Research Laboratory, 4-2-1 Nukui Kita, Koganei, Tokyo 184-8795 Japan; email: thurai@crl.go.jp

2. RADAR MEASUREMENTS

The measurements were made in February 1998, in Kashima, Japan, during a prolonged stratiform event. The radar used for these measurements operates at the same frequency as the TRMM-PR but has enhanced capability. It consists of a 2kW peak output power TWTA and a dual channel receiver for horizontal and vertical polarizations. The pulse width of 0.5 microseconds gives a range resolution of 75 meters and, moreover, over-sampling in range is possible so that the radar reflectivity can be derived at every 37.5 meters. Two data acquisition modes are available, namely, integral mode and all-hit mode. In the former case, the system records the radar reflectivity, the mean velocity and the spectrum width whilst in the latter, the pulse-by-pulse I/Q data are recorded, which enables the Doppler power spectrum to be derived. When operating in the vertically-pointing mode, the measured velocity spectra correspond to the fall velocity spectra of the hydrometeors.

The February 1998 measurements were taken in the vertically-pointing mode. Figure 1 shows the time series plot of the co-polar reflectivity. The melting layer is clearly visible at 2 km height (except at the start of the rain event), characterized by the dBZ enhancement, which gives rise to the radar bright band typically observed during stratiform events. The data below 1 km should be neglected since the range gates below this height have significant contributions from ground clutter and the transmit pulse. The latter particularly affects the range gates below 300 meters.

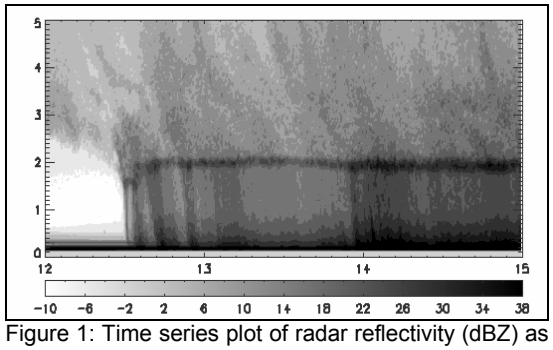

Figure 1: Time series plot of radar reflectivity (dBZ) as a function of height (km), taken on 20 Feb 1998

Co-located with the Ku-band radar was a Joss-Waldvogel disdrometer which recorded the rain drop size distribution on the ground with an integration time of 30 seconds. Figure 2a compares the dBZ derived from the disdrometer data with the radar reflectivity at

1.3 km height. The latter has been suitably time-shifted to allow for the time taken for the drops to fall. This assumed a mean fall speed of rain drops to be around 6 m/sec. The rainfall rates obtained from the disdrometer data are given in Figure 2b.

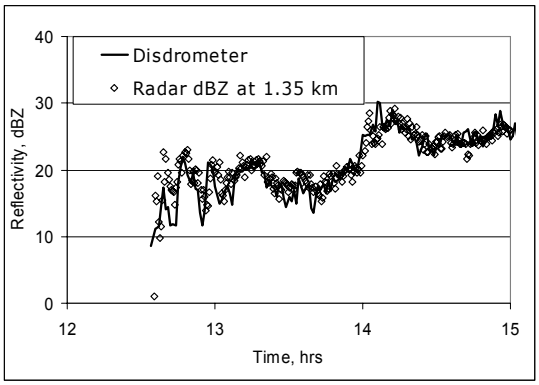

Figure 2(a): Disdrometer-derived dBZ compared with the radar reflectivity at 1.35 km (after time adjustment)

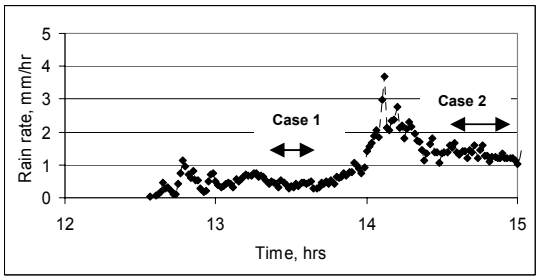

Figure 2(b): Disdrometer-derived rain fall rate, mm/hr

Excellent agreement is obtained between the radar reflectivity and the disdrometer-derived dBZ, indicating that the radar calibration is probably within 1 dB. The good correlation also indicates that the event is a 'steady-state' one. Two stable periods were chosen during this event, viz.: (1) 18-minute period between 13:24 and 13:42 and (2) 20-minute period from 14:18 to 14:38, during which the ground rainfall rate remained relatively constant. For case (1), the averaged rainfall rate was around 0.4 mm/h, i.e. drizzle, whilst for case (2), it was 1.6 mm/h, i.e. low rainfall rate. The averaged dBZ profiles for the two cases are shown as a function of height in Figure 3. Two features can be noticed:- one is that the more intense case (in relative terms) shows a bright-band peak which occurs at a height noticeably lower than the less intense one and the second is that the higher the intensity, the thicker the melting layer. Both these features are consistent with some previously reported long-term X-band radar observations of the melting layer (Fabry and Zawadski, (1995), in particular Figure 10), made in Montreal, a mid-latitude location as is the case with Kashima. Hence it is possible that the two characteristics observed within the melting layer apply to mid-latitude climates in general. We now examine if these are consistent with the N-N model predictions. A brief description of the model is given first.

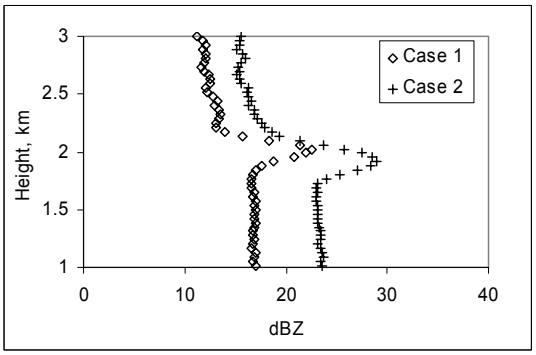

Figure 3: Averaged dBZ profiles for cases 1 and 2

3. N-N MELTING LAYER MODEL

The N-N model assumes that the flux of the particles is preserved during the melting process, i.e. the equation

$$N_S(D_S).v_S(D_S).dD_S = N_R(D_R).v_R(D_R).dD_R \quad (1)$$

is assumed to hold during the entire melting process. Here, N represents the size distribution, v the fall velocity, D the particle diameter, with S and R representing snow and rain respectively. A full description is given in Awaka et al. (1985), hence only the salient points are given here.

For an assumed drop size distribution in rain, it becomes possible to derive the equivalent size distribution at any given stage in the melting process, provided we know the relationship between the fall velocity of the melting snowflake and its diameter.

In this model, two different formulae are used to relate v_S and D_S, depending on the stage of melting. These are given by:-

$$v_S = 8.8\sqrt{(\rho_S - \rho_a)\,0.1 D_S} \quad \text{m/s for } \rho_S \le 0.3 \text{ g/cm}^3 \quad (2)$$

$$v_S = \frac{\left(v_R - v_S^0\right).\left(\rho_S^{1/3} - 0.3^{1/3}\right)}{\left(1 - 0.3^{1/3}\right)} + v_S^0 \quad \text{m/s for } \rho_S > 0.3 \text{ g/cm}^3$$

where ρ_S and ρ_a represent the density of snow and air respectively and v_S^0 is the fall speed of the melting particle when ρ_S = 0.3 g/m^3.

Using the approximations:-

$$D_S = \frac{D_R}{\rho_S^{1/3}} \quad \text{and} \quad \rho_S = \sqrt{P_W}$$

where P_W represents the volume content of water, the fall speed of each melting particle is determined. P_W is obtained from a predefined look-up table as a

function of height with respect to the top of the melting layer. In the rain region, the velocity-diameter relationship given by Atlas and Ulbrich (1971) is used for $v_R(D_R)$ in equation (1).

Having derived the size distribution of the melting particles, the radar reflectivity is computed in a manner which is analogous to rain, i.e.:-

$$Z = \int_{D_{min}}^{D_{max}} \sigma_b(D_S).N_S(D_S).dD_S \quad (3)$$

where $\sigma_b(D_s)$ is the backscatter cross section of the melting snow particle with diameter D_s. The dielectric constant is calculated from Wiener's theory and the backscatter coefficient $\sigma_b(D_s)$ is obtained using Mie scattering (for further details, refer to Awaka et al., 1985). The Doppler spectrum $S_s(v_s)$ can be derived in an analogous way using:-

$$S_S(v_S)\,dv_S = N_S(D_S).\sigma_b(D_S).dD_S \quad (4)$$

where $N_S(D_S)$ is calculated using equation (1). There is one other factor which needs to be taken into consideration, namely the correction term for the fall velocity due to air density change with height. In this study, a US standard atmosphere has been assumed.

4. MODEL COMPARISONS

4.1 *Reflectivity-height profiles*

The model predictions of dBZ-height variations are given in Figure 4 for cases (1) and (2), as solid and dotted lines respectively. These were obtained using the fitted parameters to the averaged drop size distribution as input to the model for the two cases. The fitted DSD parameters assuming an exponential distribution are given in Table 1 where the exponential function is given by the expression:

$$N_R(D_R) = N_0\ exp\left(-3.67\ \frac{D_R}{D_0}\right) \quad (5)$$

D_0 being the median mass diameter and N_0, being the intercept parameter of the full DSD, $N_R(D_R)$, in rain.

TABLE 1: DSD parameters from the disdrometer data

Parameter	Case 1	Case 2
N_0	3510	7221
D_0 mm	0.91	0.96
Rainrate, mm/h	0.41	1.6

The model predicted dBZ profiles do not show the same trend as was observed with the Ku-band radar measurements. For example, the bright-band peak occurs at almost the same height for the two predicted curves and their thickness remains more or less the same. Furthermore, in both cases the model predicts thicker melting layer than the data. These dissimilarities perhaps point to some limitations of the N-N model, at least for weak stratiform rain in mid-latitude regions. It's worth noting again that the Ku-band radar dBZ profiles for cases 1 and 2 are consistent with the long-term characteristics of the melting layer in Montreal, previously reported by Fabry and Zawadski (1985), which also show the intensity dependence of the melting layer thickness and the height of the bright band peak.

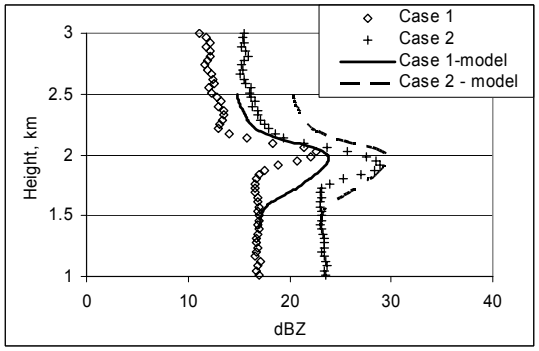

Figure 4: Averaged dBZ profiles for cases 1 and 2 compared with the N-N model predictions

4.2 *Fall-velocity spectra*

The measured spectra at various, selected, heights within the melting layer are shown in Figures 5(a) and 5(b) for cases (1) and (2). The curves corresponding to 2.3 km represent the spectra in the snow region, both being narrow spectra, with a peak velocity of around 1.5 m/sec. At lower heights, the measured spectra become broader and their peak positions shift to higher velocities, indicating the various stages of melting. For case (1), the spectra at 1.6 km and 1.8 km heights are similar, indicating that the melting gets completed by 1.8 km, whereas for case (2), the melting process takes longer, in fact down to 1.6 km height. For both cases, the spectra at 1.6 km correspond to the fall velocity distribution in rain.

Over-plotted on the graphs in Figures 5(a) and 5(b) are the predicted spectra from the N-N model for (i) snow, (ii) bright-band peak and (iii) rain regions. Qualitatively, the two sets of curves agree with each other in that the model predicts similar range of velocities to the measured data for all three types of hydrometeors. However, the corresponding heights at which these spectra are compared do not match. In accordance with Figure 4, the model spectra correspond to 2.5 km, 2.0 km and 1.5 km heights respectively, which are somewhat different from those of the measured data, particularly for case (1). Given the fact that the N-N model has a fixed height variation of the water content and the so called 'form factor' (used to calculate the dielectric constant of the ice/water/air mixture), it may be possible to alter the model by using an additional term relating the bright-

band thickness to the dBZ in rain. One possibility is to use a power-law formula, for example, one that is similar to the expression given in Fabry and Zawadski (1985). This needs to be considered since the model-derived attenuation will affect the path integrated attenuation used in the rain retrieval algorithms. The effect will be even higher at Ka-band, 35 GHz being the frequency proposed for the additional radar on-board the TRMM follow-on mission (Global Precipitation Measurement Mission).

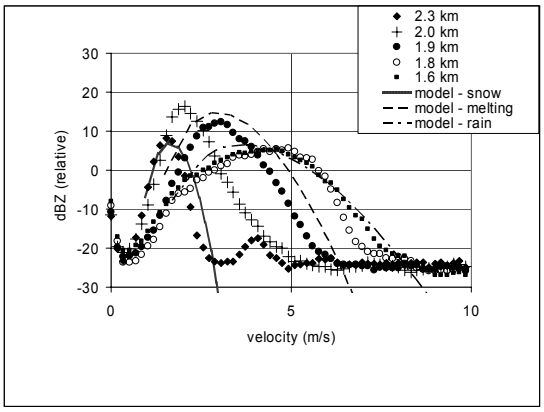

Figure 5(a): Fall velocity spectra for case 1 for various heights within the melting layer (points) compared with the N-N model predictions (lines) for 0.4 mm/h

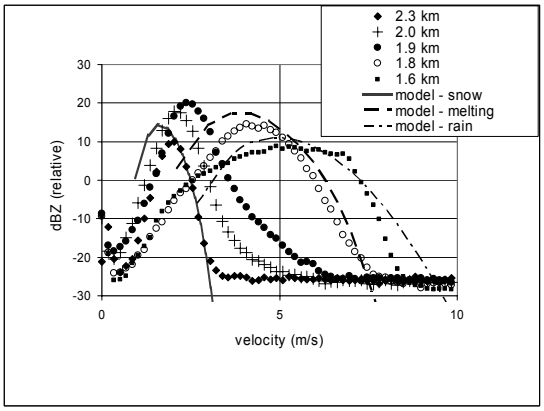

Figure 5(b): Same as Figure 5(a), but for case 2 with 1.6 mm/h rainfall rate.

5. CONCLUSIONS

Ku-band radar measurements of a prolonged weak, stratiform rain in Kashima, Japan, taken in the vertically pointing mode are reported here. The radar measured the full Doppler spectrum with a range resolution of 37.5 m. Fall velocity spectra show a narrow distribution in the snow region with a mean velocity of 1.5 m/s which gets wider as the melting progresses. The velocity spectra in the rain region are consistent with the disdrometer-derived distribution, co-located with the radar.

The melting layer spectra were compared with the Non-coalescence – Non-break up melting layer model predictions. Although the range of velocities within the melting layer agrees well with the data, the melting layer thickness shows significant differences. The measurements indicate that the bright-band thickness is intensity dependent whereas the model predictions do not show any appreciable variation with the radar reflectivity in the rain region just below the bright band. This limitation of the model may need to be addressed for future missions such as the Global Precipitation Measurement (GPM) mission which will include Ku as well as Ka radar measurements over mid-latitude regions.

REFERENCES

Atlas, D., and C. W. Ulbrich, 1977: Path- and area-integrated rainfall measurement by microwave attenuation in the 1-3 cm band., *J. Appl. Meteor.*, **16**, 1322-1331.

Awaka, J., Y. Furuhama, M. Hoshiyama, and A. Nishitsuji, 1985: Model calculations of scattering properties of spherical bright-band particles made of composite dielectrics, *J. Radio Research Lab.*, **32**(136), 73-87.

D'Amico, M., A.R. Holt, and C. Capsoni, 1998: An anisotropic model of the melting layer, *Radio Sci.,* **33**, 535-552.

Fabry, F., and I. Zawadski, 1995: Long term radar observations of the melting layer of precipitation and their interpretation. *J. Atmos. Sci.*, **52**(7), 838-851.

Hardaker, P., A. Holt, and C. G. Collier, 1995: A melting layer model and its use in correcting for the bright band in single-polarisation radar echoes, *Quart. J. Royal Met. Soc.*, **121**, 495-525.

Iguchi, T., T. Kozu, R. Meneghini, J. Awaka, and K. Okamoto, 2000: Rain profiling algorithm for TRMM Precipitation Radar, *J. Appl. Meteor.*, **39**(12), 2038-2052.

Liao, L., R. Meneghini, and T. Iguchi, 2002: Bright-band modeling of air/space-borne microwave radars, IEEE *International Geosci. and Remote Sens. Symp*, Toronto, Canada, 278-280.

Russchenberg, H.W.J., and L. P. Ligthart, 1996: Backscattering by and propagation through the melting layer of precipitation: a new polarimetric model, *IEEE Trans. Geosci. Remote Sens.,* **34**, 3-14.

Thurai, M., T. Iguchi, J. W. F. Goddard, J. T. Ong, and J. Awaka, 2003: Melting layer model evaluation in Singapore, *International Conference on Antennas and Propagation*, IEE Conference Publication No **491**, Exeter, United Kingdom, 1.357-1.360.